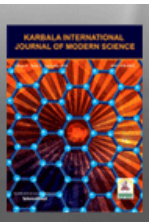

Karbala International Journal of Modern Science

Volume 10 | Issue 1 Article 9

Synthesis and Characterization of Renewable Heterogeneous Catalyst ZnO Supported Biogenic Silica from Pineapple Leaves Ash for Sustainable Biodiesel Conversion

Nadila Pratiwi
Department of Chemistry, Faculty of Mathematics and Natural Science, Universitas Negeri Makassar, Makassar, South Sulawesi, Indonesia;

Suriati Eka Putri
Department of Chemistry, Faculty of Mathematics and Natural Science, Universitas Negeri Makassar, Makassar, South Sulawesi, Indonesia, ekaputri_chem@unm.ac.id

Yulia Shinta
Department of Chemistry, Faculty of Mathematics and Natural Science, Universitas Negeri Makassar, Makassar, South Sulawesi, Indonesia;

Arya Ibnu Batara
Department of Mechanical Engineering, Faculty of Engineering, Universitas Negeri Makassar, Makassar, South Sulawesi, Indonesia

Diana Eka Pratiwi
Department of Chemistry, Faculty of Mathematics and Natural Science, Universitas Negeri Makassar, Makassar, South Sulawesi, Indonesia

See next page for additional authors

Recommended Citation

Pratiwi, Nadila; Putri, Suriati Eka; Shinta, Yulia; Batara, Arya Ibnu; Pratiwi, Diana Eka; Rahman, Abd; Ahmad, Nur; and Heryanto, Heryanto (2024) "Synthesis and Characterization of Renewable Heterogeneous Catalyst ZnO Supported Biogenic Silica from Pineapple Leaves Ash for Sustainable Biodiesel Conversion," *Karbala International Journal of Modern Science*: Vol. 10 : Iss. 1 , Article 9.
Available at: https://doi.org/10.33640/2405-609X.3343

Synthesis and Characterization of Renewable Heterogeneous Catalyst ZnO Supported Biogenic Silica from Pineapple Leaves Ash for Sustainable Biodiesel Conversion

Abstract

This study reports on the first case of the low-cost and environmentally friendly ZnO/SiO2 heterogeneous catalyst from pineapple leaves ash (PLA). Catalyst shows excellent performance in catalyzing the transesterification of waste cooking oil (WCO) with methanol for biodiesel conversion. This study focuses on assessing the influence of Zn content on physicochemical characteristics, using XRD, FTIR, SEM, and N2 adsorption-desorption methods. In addition, three different Zn content levels (20, 25, and 30 %wt) were applied. The results showed that all ZnO/SiO2 samples exhibited characteristics suitable for use as catalyst with an average crystallite size of 31.83-34.15 nm, and a surface area of 88.97 m2/g to 93.41 m2/g. Importantly, the sample shows efficient catalytic activity for conversion of biodiesel from WCO with the largest conversion using a ZnO/SiO2-30 catalyst of 96.17% with the carbon chain of C12-C20. The optimum reaction conditions used 3 g of ZnO/SiO2-30, reaction time 6 hours at 57.5 oC and WCO to methanol ratio of 3:1 with a yield of 98.62%. The resulting catalyst has extraordinary durability up to sixth cycles. It shows that the material has the potential to be a renewable catalyst from sustainable resources. The ZnO/SiO2 catalyst production using PLA for biodiesel production from WCO represents the potential for using agricultural waste into valuable materials in future energy.

Keywords

catalyst, silica, pineapple, biodiesel

Authors

Nadila Pratiwi, Suriati Eka Putri, Yulia Shinta, Arya Ibnu Batara, Diana Eka Pratiwi, Abd Rahman, Nur Ahmad, and Heryanto Heryanto

RESEARCH PAPER

Synthesis and Characterization of Renewable Heterogeneous Catalyst ZnO Supported Biogenic Silica from Pineapple Leaves Ash for Sustainable Biodiesel Conversion

Nadila Pratiwi [a], Suriati E. Putri [a,*], Yulia Shinta [a], Arya I. Batara [b], Diana E. Pratiwi [a], Abd Rahman [c], Nur Ahmad [d], Heryanto Heryanto [e]

[a] Department of Chemistry, Faculty of Mathematics and Natural Science, Universitas Negeri Makassar, Makassar, South Sulawesi, Indonesia
[b] Department of Mechanical Engineering, Faculty of Engineering, Universitas Negeri Makassar, Makassar, South Sulawesi, Indonesia
[c] Department of Chemistry, King Fahd University of Petroleum & Minerals, Dhahran 31261, Saudi Arabia
[d] Graduate School, Faculty of Mathematics and Natural Sciences, Sriwijaya University, South Sumatera, Indonesia
[e] Department of Physics, Faculty of Mathematics and Natural Sciences, Hasanuddin University, Makassar, South Sulawesi, Indonesia

Abstract

This study reports on the first case of the low-cost and environmentally friendly ZnO/SiO_2 heterogeneous catalyst from pineapple leaves ash (PLA). Catalyst shows excellent performance in catalyzing the transesterification of waste cooking oil (WCO) with methanol for biodiesel conversion. This study focuses on assessing the influence of Zn content on physicochemical characteristics, using XRD, FTIR, SEM, and N_2 adsorption−desorption methods. In addition, three different Zn content levels (20, 25, and 30 %wt) were applied. The results showed that all ZnO/SiO_2 samples exhibited characteristics suitable for use as catalyst with an average crystallite size of 31.83−34.15 nm, and a surface area of 88.97 m^2/g to 93.41 m^2/g. Importantly, the sample shows efficient catalytic activity for conversion of biodiesel from WCO with the largest conversion using a ZnO/SiO_2-30 catalyst of 96.17 % with the carbon chain of C_{12}−C_{20}. The optimum reaction conditions used 3 g of ZnO/SiO_2-30, reaction time 6 h at 57.5 °C and WCO to methanol ratio of 3:1 with a yield of 98.62 %. The resulting catalyst has extraordinary durability up to sixth cycles. It shows that the material has the potential to be a renewable catalyst from sustainable resources. The ZnO/SiO_2 catalyst production using PLA for biodiesel production from WCO represents the potential for using agricultural waste into valuable materials in future energy.

Keywords: Catalyst, Silica, Pineapple, Biodiesel

1. Introduction

Fuel serves as a crucial global requirement for transportation and industrial sectors, is primarily derived from fossil fuels. However, burning fossil fuels results in harmful emissions including nitrogen oxides (NO_x), sulfur oxides (SO_x), carbon monoxide (CO), carbon dioxide (CO_2), and other pollutants. Subsequently, fossil fuel is also non-renewable, and the energy demand for this fuel is estimated to increase by 2 % per year [1]. To address these challenges, researchers are exploring alternative fuel synthesis from renewable and eco-friendly sources, with biodiesel emerging as a promising option [2,3].

Biodiesel is a promising alternative energy source, with renewable raw materials sourced from biomass and various vegetable oils, such as soybean oil [4], palm oil [5], WCO [6], castor oil [7], sunflower oil [8], which have been studied intensively in recent years.

Received 22 November 2023; revised 29 December 2023; accepted 21 January 2024.
Available online 22 February 2024

* Corresponding author.
E-mail address: ekaputri_chem@unm.ac.id (S.E. Putri).

https://doi.org/10.33640/2405-609X.3343

Compared to petroleum-diesel, biodiesel fuel has a number of advantages, such as being free of sulfur and aromatic compounds, non-toxic, renewable, and has a high flash point, so it can reduce air pollution significantly [9].

Several methods can be used in biodiesel production process, such as supercritical fluid method, pyrolysis, micro-emulsion, and transesterification method [3,10]. Among these methods, the transesterification is an effective, reliable, and the most widely used method, because it does not require a large amount of energy and can be carried out at low temperatures and pressure [11]. Additionally, the transesterification method for biodiesel has a straightforward procedure and a high biodiesel efficiency [12]. The transesterification method is a chemical reaction that requires alcohol to break the triglyceride chains in the raw materials used, usually biomass, vegetable oils, or animal oils. This process results in the formation of biodiesel or methyl esters and glycerol in the end product [2]. Commonly, methanol and ethanol are used for this purpose due to their high reactivity and cost-effectiveness, leading to the production of fatty acid methyl ester (FAME) and fatty acid ethyl ester (FAEE), respectively [13]. Therefore, methanol is often used to produce biodiesel due to its lower price and higher reactivity [12], and in our study, a catalyst was used to accelerate the reaction.

The type of catalyst currently under development in several industrial processes is the heterogeneous catalyst. In the context of biodiesel conversion, heterogeneous catalyst is gaining prominence as replacements for alkaline or acidic homogeneous catalyst, presenting challenges and opportunities for sustainable development [14]. High activity level, low cost, reusability, and recovery are some of catalyst properties considered for an economical and sustainable process [15]. Additionally, physicochemical properties such as surface area, surface alkalinity/acidity, and pore distribution, are some of the characteristics that influence catalyst performance [16,17]. Several studies showed the effectiveness of Lewis acid catalyst in the transesterification mechanism; some transition metal salts show that the Lewis acid site strength is $Sn^{2+} >> Zn^{2+} > Al^{3+}$ [18].

The most widely used metal oxide is ZnO because it is capable of producing a fairly large percent yield of biodiesel, as reported by several previous studies [9,19]. To improve catalyst performance, transition metals are generally impregnated into a porous solid support. Previous investigations reported several catalyst supports that have been used in biodiesel conversion process such as zeolite, activated carbon, and alumina, as well as mesoporous silica (MCM) [20–22]. However, cost is an important factor to consider, given the high cost and multiple processes involved in the synthesis of these minerals. The development of sustainable and affordable heterogeneous catalysts is necessary so SiO_2-based low-cost materials have been widely developed to promote economic solutions [23]. Because biogenic silica is easily produced and modifiable, it makes sense as a catalyst for this purpose [24]. Several agricultural wastes that have been used as sources of biogenic silica include rice husk ash of 28.12 %, bamboo leaves of 27.65 %, and salacca leaves of 27.98 % [16,24,25].

The use of biogenic silica as a support for the ZnO catalyst has previously investigated using salacca leaves ash, producing a biodiesel yield of 98.44 % [16]. One of the agricultural wastes that is quite abundant in our city is pineapple leaves. From previous investigations, PLA contains quite high silica, namely 34.13 % [26]. The utilization of pineapple leaves ash as a heterogeneous catalyst in the biodiesel production process has been studied previously which resulted in a very superior conversion percentage of soybean oil of 98 % [27]. Thus, it has the potential to be used as a supporting ZnO as catalyst for biodiesel conversion [28]. In this research, ZnO/SiO_2 was synthesized using biogenic silica derived from PLA. To the best of authors' knowledge, this is the first case study utilizing biogenic silica from PLA as a ZnO catalyst support for biodiesel conversion.

There are various feedstocks (oil sources) for producing biodiesel, including waste oils (e.g., waste edible oil (WEO) or WCO), animal fats, microalgae oils, and vegetable oils [9]. Used cooking oil in restaurants and homes can be considered WCO. In biodiesel production, more than 70 % of the costs are related to the oil source. Therefore, the use of low quality oils such as non-edible oils and WCO can be a better oil source for biodiesel production because these raw materials can provide economic feasibility of the biodiesel generation process [12]. Consequently, WCO was selected as a biodiesel source since it is non-edible, less expensive than refined oil [29], and can lessen environmental effects from inappropriate disposal [30], considering the annual global consumption of approximately 5 million tons of refined oil [8]. Based on previous research investigations, WCO has been widely used as a biodiesel feedstock using several types of heterogeneous catalysts such as Fe_3O_4/SiO_2@ZnO [31], Al-doped ZnO [32], AC@ZnO/NiO [15]. Apart from that, the use of agricultural waste as a raw catalyst for the production of biodiesel from WCO has also

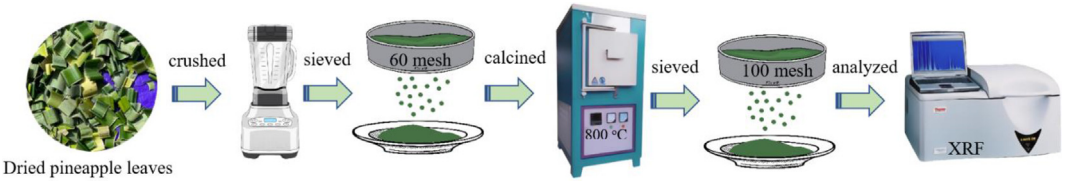

Fig. 1. The preparation PLA illustration.

been carried out previously using walnut shell/sawdust [33], sawdust [34], and date seeds [15]. The use of PLA as a raw catalyst for biodiesel conversion from WCO has never been done before, so this study is a new innovation.

2. Materials and methods

2.1. Materials

All chemicals used are of pro analytical grade, such as hydrochloric acid (HCl, Merck), sodium hydroxide (NaOH, Merck), potassium hydroxide (KOH, Merck), zinc acetate dihydrate ($Zn(CH_3COO)_2.2H_2O$, Merck), zinc oxide (ZnO, Merck CAS Number 1314-13-2), potassium iodide (KI, Merck), chloroform (CH_3Cl_3, Merck), Hanus solution, methanol (CH_3OH, Merck), neutral alcohol 95 %, phenolphthalein indicator ($C_{20}H_{14}O_4$, Merck), starch.

The WCO as feedstock for biodiesel conversion was obtained from a cake shop in Tamalate District, Makassar City of Indonesia, with three to four uses. The WCO used has a density of 0.91 g/cm^3, acid value 9.239 mg-KOH/g, FFA content 4.926 %, and saponification number of 168.32 mg/g.

2.2. Preparation of PLA

Pineapple leaves sourced from waste in Binamu District, Jeneponto Regency, South Sulawesi, Indonesia, were dried, crushed to a smooth texture, sieved through a 60-mesh, and calcined at 800 °C for about an hour. The powder obtained through 100-mesh sieving, was subjected to XRF analysis to determine silica content. The preparation of PLA is described in Fig. 1.

2.3. The silica extraction from PLA

The process of extracting silica from pineapple leaves involved being mixed with a 4 M NaOH solution and refluxing the mixture for approximately 4 h. After the refluxed filtrate reached pH 8, a silica gel was created by gradually titrating it with a standard 0.5 M HCl solution. The silica gel was then separated from the filtrate by decantation, and the gel was neutralized with distilled water. Additionally, it was filtered and dried at 60 °C. Fig. 2 illustrates the method used for silica extraction from PLA.

2.4. The ZnO/SiO_2 synthesis

The ZnO/SiO_2 composite was synthesized using the resulting silica gel. Water is used to dissolve the precursor solution $Zn(CH_3COO)_2.2H_2O$. Following that, it was mixed with silica gel to form a colloid, underwent centrifugation, dried at 80 °C, and was subsequently calcined for 2 h at 500 °C (Fatimah

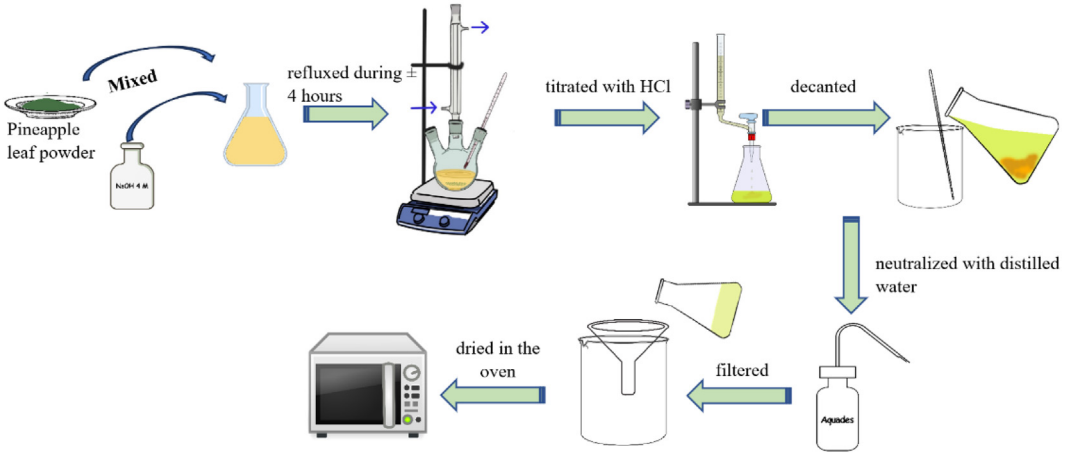

Fig. 2. The illustration of extraction silica from PLA.

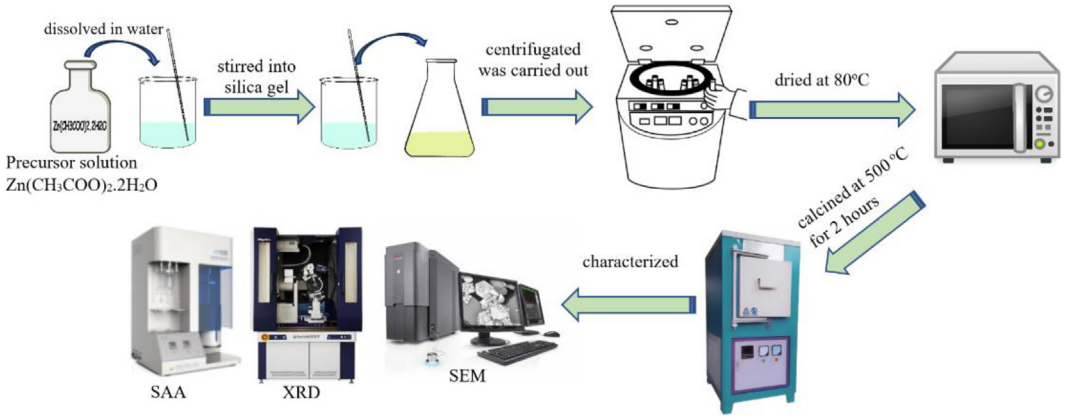

Fig. 3. The schematic diagram of synthesis ZnO/SiO_2.

et al., 2022). ZnO concentration was altered at 20, 25, and 30 weight percent to investigate the impact of ZnO on the catalytic characteristics. The resulting samples were labelled ZnO/SiO_2-20, ZnO/SiO_2-25, as well as ZnO/SiO_2-30, respectively. Fig. 3 shows the method of ZnO/SiO_2 synthesis.

2.5. The ZnO/SiO_2 catalytic activity

The catalytic activity of the catalyst was assessed through transesterification reaction between WCO and methanol using ZnO/SiO_2. The FFA in WCO is quite high, content over 2.5 % so a pretreatment steps are needed necessary before the transesterification process [35]. The pretreatment steps carried out consist of degumming and esterification steps. Degumming is one steps of the purification process which aims to remove the gum and slime in WCO by using HCl with a volume of 0.5 %. Then add NaOH 0.5 % and 200 mL of water at 120 °C for neutralize the pH and dissolve the salts in WCO. The next pretreatment was esterification which aims to reduced the FFA in WCO using H_2SO_4 0.05 % from the total volume of WCO at a temperature of 60 °C for 1 h, then settled for 24 h. After esterification, the FFA content decreased to 1.84 %.

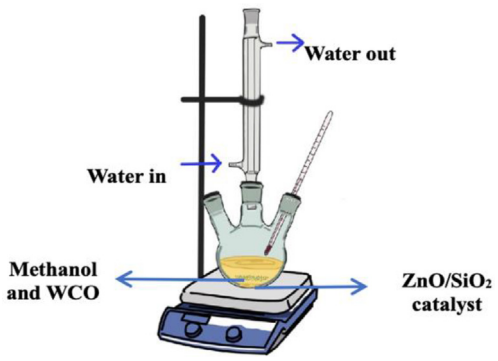

Fig. 4. The schematic for the transesterification reaction.

Subsequently, the transesterification reaction between WCO and methanol (3:1) using 1 g of biogenic SiO_2, pure ZnO, and ZnO/SiO_2. All reactions were carried out in round-bottom flask fitted with a reflux condenser, as shown in Fig. 4. The reaction took place for 6 h at a temperature of 60 °C [16]. The reaction conditions used were based on previous study [16], to determine which samples would be used in the optimization condition. The reaction mixture was put in a separating funnel, and the methyl ester (biodiesel) and glycerol were allowed to fully separate over 12 h. After the final product is filtered, a titrimetric quantitative analysis is performed on the biodiesel to determine its density, acid number, saponification number, iodine number, as well as cetane number. The methyl ester product with the greatest conversion and meeting the SNI 7182:2015 standard was subjected to qualitative analysis using GC–MS.

For the process of optimizing reaction conditions, a ZnO/SiO_2 composite with the largest conversion percentage was used. The various reaction conditions are regulated by referring to the Central Composite Design (CCD) from Response Surface Methodology (RSM). This is to identify the influencing parameters and optimal conditions for catalytic conversion. The parameter variations chosen for optimization are as follows: catalyst dosage, reaction time, and reaction temperature. Yield (%) is selected as the response to the reaction. Parameters are selected after optimization on a wider range of variables. In addition, the WCO to methanol ratio was not selected as an important factor due to initial optimization; The results show that higher results were obtained with the 3:1 ratio and did not significantly increase at the 2:1 and 4:1 ratios. Therefore,

Table 1. The XRF analysis of PLA and biogenic silica.

Composition	Content (wt.%)	
	PLA	Biogenic silica
CaO	41.30	30.72
SiO_2	37.68	50.71
K_2O	11.98	10.21
P_2O_5	4.54	4.14
Cl	4.05	3.73
CuO	0.193	0.082
Rb_2O	0.122	0.091
Nb_2O_5	0.048	0.012
MoO_3	0.031	0.011
In_2O_3	0.0194	0.294
Sb_2O_3	0.0169	–
SnO_2	0.0161	–

all experiments were carried out with a WCO and methanol ratio of 3:1.

2.6. Reusability of ZnO/SiO_2

The reusability test of catalyst involves recycling the used catalyst for use in subsequent cycles. The recycling process involved washing the catalyst in methanol for an hour while agitating it, and followed by driging ried for 6 h at 100 °C, for reduces the amount of organic compounds that poison the catalyst [27].

2.7. Instrumentation

X-ray Fluorescence (XRF) Spectrometers from Thermo Fisher Scientific, featuring an X-ray vacuum path with an effective stationary size of 13.0 mm, as well as an effective K alpha area of 132.7 mm^2, were used to analyze the metal oxide content of pineapple leaves before and after extraction. A powder X-ray diffractometer (XRD, Shimadzu 7000) with CuKα radiation (λ = 1.5405 Å) operating at a configuration scanning range of 10–80 was used to assess the crystallinity of CdS. The Debye–Scherrer formula was used to determine the size of the crystallite domain. FTIR (IR Prestige-21 Shimadzu) was carried out using the transmittance method to identify functional groups of ZnO/SiO_2. Furthermore, the spectrum was recorded at a wavelength interval of 3800 to 400 cm^{-1}. Then, for determine the surface are and pore distribution using SAA (Quantachrome Nova 4200e) at 250 °C 3 h for gas departure, and 273 K for the bath temperature, the surface area and pore properties of ZnO/SiO_2 were ascertained. Textural qualities were ascertained using Brunauer-Emmet-Teller (BET) method. Pore volume and surface area were computed. The entire pore volume was represented by the t-plot approach using the total gas

Fig. 5. The physical appearance of (a) PLA and (b) biogenic silica from PLA.

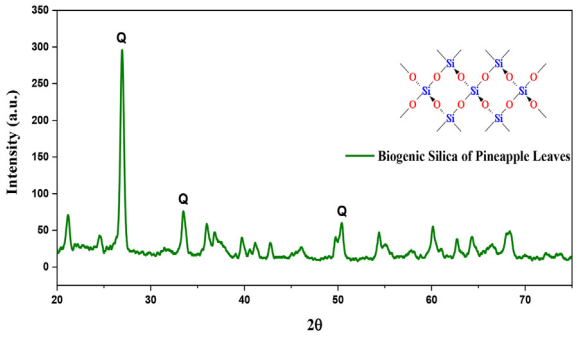

Fig. 6. The XRD pattern of biogenic silica from PLA.

adsorbed at a relative pressure of P/Po = 0.99. With an accelerating voltage of 130 kV, a scanning electron microscope (JEOL JSM 6063LA) was used to record the ZnO/SiO_2 surface morphology.

3. Results and discussions

In the synthesis of catalyst materials using natural resources, the metal oxide content is a significant consideration. Table 1 shows the findings of the XRF study conducted to determine the metal oxide concentration of pineapple leaves. The physical appearance of pineapple leaves preparation results is brownish green, as shown in Fig. 5a.

XRF analysis shows that the amount of SiO_2 in PLA is 37.68 % with the largest impurity being CaO at 41.30 %. The SiO_2 content increased to 50.71 % after extraction of PLA using NaOH with the physical appearance as shown in Fig. 5b, the results obtained were higher than previous study [28]. Therefore, PLA can be used as a source of biogenic silica in the synthesis of heterogeneous catalyst.

The biogenic silica phase was analyzed using XRD, as shown in Fig. 6. Comparing the results with

Table 2. The XRF analysis of the ZnO/SiO_2 catalyst.

Sample	SiO_2 (%)	ZnO (%)	Impurity (CaO)
ZnO/SiO_2-20	65,28	24,77	9,94
ZnO/SiO_2-25	66,12	30,27	3,61
ZnO/SiO_2-30	64,16	34,35	1,49

Table 3. The average crystal size of ZnO/SiO_2.

2-theta (°)	ZnO/SiO_2-20		ZnO/SiO_2-25		ZnO/SiO_2-30	
	Crystallite size (nm)	The average crystallite size (nm)	Crystallite size (nm)	The average crystallite size (nm)	Crystallite size (nm)	The average crystallite size (nm)
31.39	30.95	31.83	30.94	33.39	31.14	34.15
34.06	30.29		30.27		30.57	
35.89	30.14		29.99		31.29	
44.11	39.73		39.67		39.97	
47.21	31.18		31.15		31.65	
56.29	29.78		30.16		29.96	
62.57	28.32		28.98		28.18	
64.48	35.11		35.05		35.85	
67.68	30.39		31.06		30.96	
68.81	32.52		33.46		32.86	

JCPDS No. 46–1045 reveals that the sample's phase corresponds to the quartz phase, identifiable by characteristic peaks at 2θ 26.94°, 33.46°, and 50.39°. The results obtained are different from biogenic silica from bamboo ash, which produces an amorphous phase [25].

3.1. Physicochemical characterizations of ZnO/SiO_2

The results of analysis using XRF were carried out to determine the ZnO content in each catalyst with varying amounts of ZnO, as described in Table 2. The findings showed that the highest ZnO content of 34.35 % of ZnO/SiO_2-30. These findings are consistent with a prior study that found that raising the ZnO content may be achieved by raising the $Zn(CH_3COO)_2.2H_2O$ solution's concentration as a precursors [16]. There is a significant relationship between the active side of the resulting catalyst and the increase in the amount of precursor. Determination of the upper limit of active side addition on the catalyst, which may indicate a saturation point, requires further investigation into the relationship between increasing precursors and the percentage of active sides on the generated catalyst. In this study, only up to 30 % was carried out because it refers to previous research which also used biogenic silica as a support for the ZnO catalyst, at precursor concentrations of 25 % and 30 % the surface acidity of the catalyst did not increase [16].

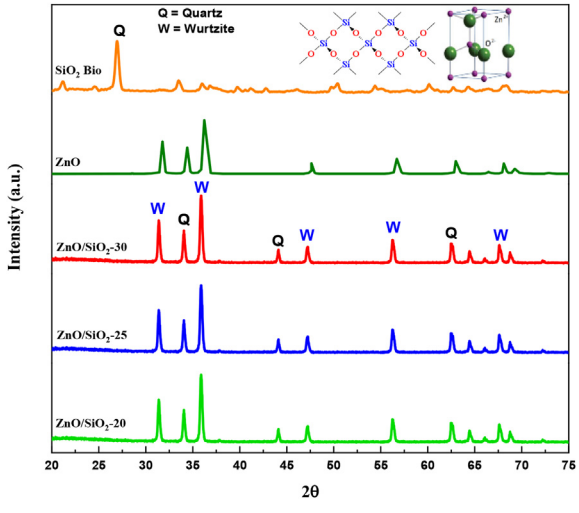

Fig. 7. The XRD pattern of ZnO/SiO_2 with various concentration.

To determine the ZnO phase in the sample, analysis using XRD was carried out as shown in Fig. 7. Based on the results, it shows the phase in the sample is the wurtzite phase with a typical peak at 2θ 31.39°; 34.06°; 35.89°; 44.11°; 47.21°; 56.29°; 62.57°; 64.48°; 67.68°; and 68.81°. This corresponds to the standard ZnO phase (JCPDS No. 36–1451), which has a hexagonal wurtzite polycrystalline structure.

The results obtained are in line with the previous study which showed the existence of a hexagonal structure in ZnO crystals synthesized using the coprecipitation method [36]. The results obtained differ from previous studies which produced spherical and hexagonal zinc oxide phases responsible for all diffraction peaks because they have a good crystalline particle structure, as seen from the narrow and strong diffraction peaks [37]. Furthermore, these results are in line with a previous study

Table 4. Surface area and pore distribution analysis (correspond from Fig. 11).

Sample	Surface area (m^2/g)	Volume @STP (cc/g)	Pore distribution (Å)
SiO_2 biogenic	59.12	0.19	0.32
ZnO	51.43	0.22	0.28
ZnO–SiO_2-20	88.97	0.14	0.33
ZnO–SiO_2-25	93.25	0.09	0.33
ZnO–SiO_2-30	93.41	0.07	0.39

that investigated ZnO–SiO_2 fabrication through the gas phase method using spray pyrolysis, showing a hexagonal wurtzite phase crystal structure [38].

In fact, wurtzite ZnO which is characterized by a hexagonal structure, exhibits diverse features that significantly affect its catalytic activity. The crystal sides exposed on the surface have different surface energies, creating specific sites with varying chemical reactivity [39]. Certain facets can exhibit a higher density of active sites that are important for catalytic reactions, thus impacting the overall catalytic performance. Additionally, the presence of defects, such as oxygen vacancies, in the wurtzite phase serve as catalytically active sites, altering the electronic structure and affecting the material's involvement in redox reactions [19]. The hexagonal lattice arrangement offers specific binding sites for the adsorption of reactant molecules, and the strength and geometry of this adsorption can determine the reaction pathway and catalytic efficiency [39]. Hexagonal symmetry introduces anisotropic properties, where different crystallographic directions exhibit varying reactivity, providing a means to tailor catalytic activity for specific reactions [36]. Furthermore, the ZnO wurtzite enhances catalytic performance by exposing the majority of active sites due to the increased surface area (presented in Table 4), making the structured material a more effective catalyst compared to its bulk counterparts.

The diffractogram pattern resulting from XRD analysis of ZnO/SiO_2 shows sharper and more intense peak broadening. This can be attributed to the average size (D) of CdS crystals calculated using the Debye Scherrer Equation (1) [40–42].

$$D_s = \frac{k\lambda_{Cu}}{\beta \cos\theta} \tag{1}$$

In this case, θ is the diffraction angle, β is the FWHM of the diffraction peaks, and l is the wavelength of the X-rays, which is defined as 1.54 $\mathring{A}$. The shape factor (k), or constant, is ~0.98 for hexagonal system. Where k is a dimensionless unit that varies with the type of crystal structure often used for particles of unknown size [43,44]. For some specific structural conditions, it has been shown that the

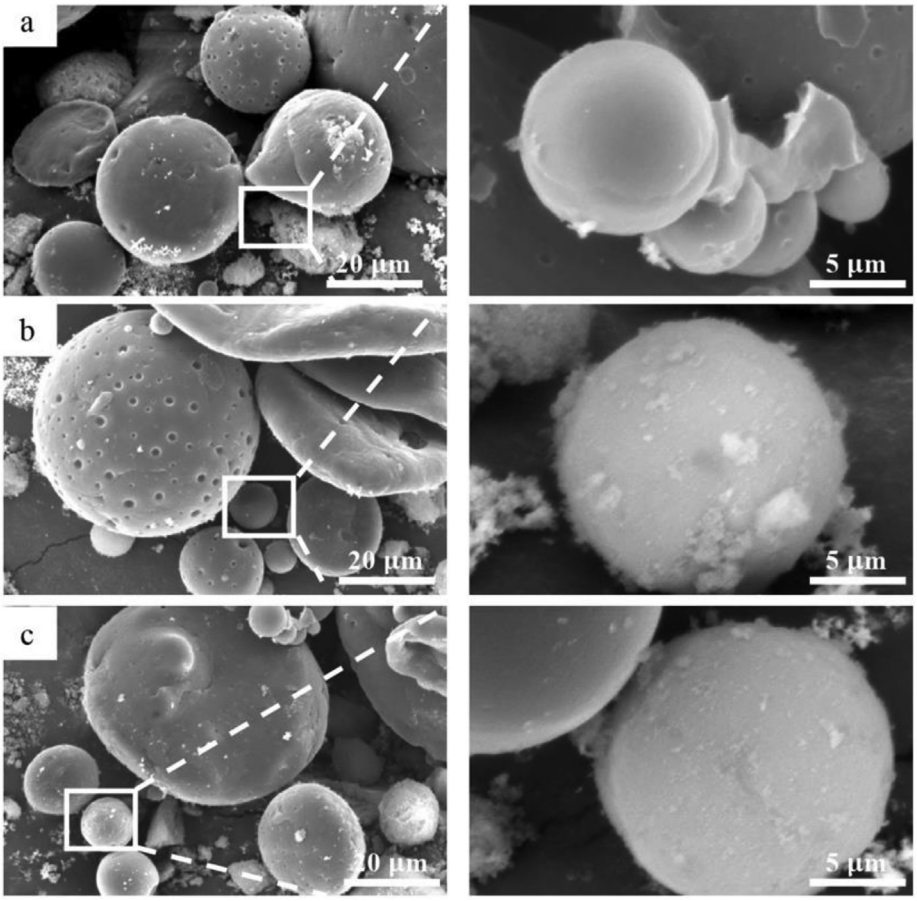

Fig. 8. The SEM images of (a) ZnO/SiO_2-20, (b) ZnO/SiO_2-25, dan (c) ZnO/SiO_2-30 with the magnification of 1000× (left) and 5000x (right).

value of *k* can range from 0.89 for spherical particles to 0.94 for cubic particles.

Table 3 presents the results, which can be observed that the ZnO contributes insignificantly to the *D*. The higher the ZnO content, the higher the average *D*. The outcomes are consistent with the pattern of earlier studies that employed salacca leaves and bamboo leaves ash as sources of biogenic silica [16,45]. The higher concentration of ZnO precursor in the synthesis process affects the deposition rate, which will influence the growth of crystal size, and will also speed up the distribution of ZnO in the sol–gel process.

Evaluation of the surface morphology of the ZnO/SiO_2 catalyst was carried out using SEM, as shown in Fig. 8. The results show that catalyst's crystals exhibit uniformity, forming spherical structures.

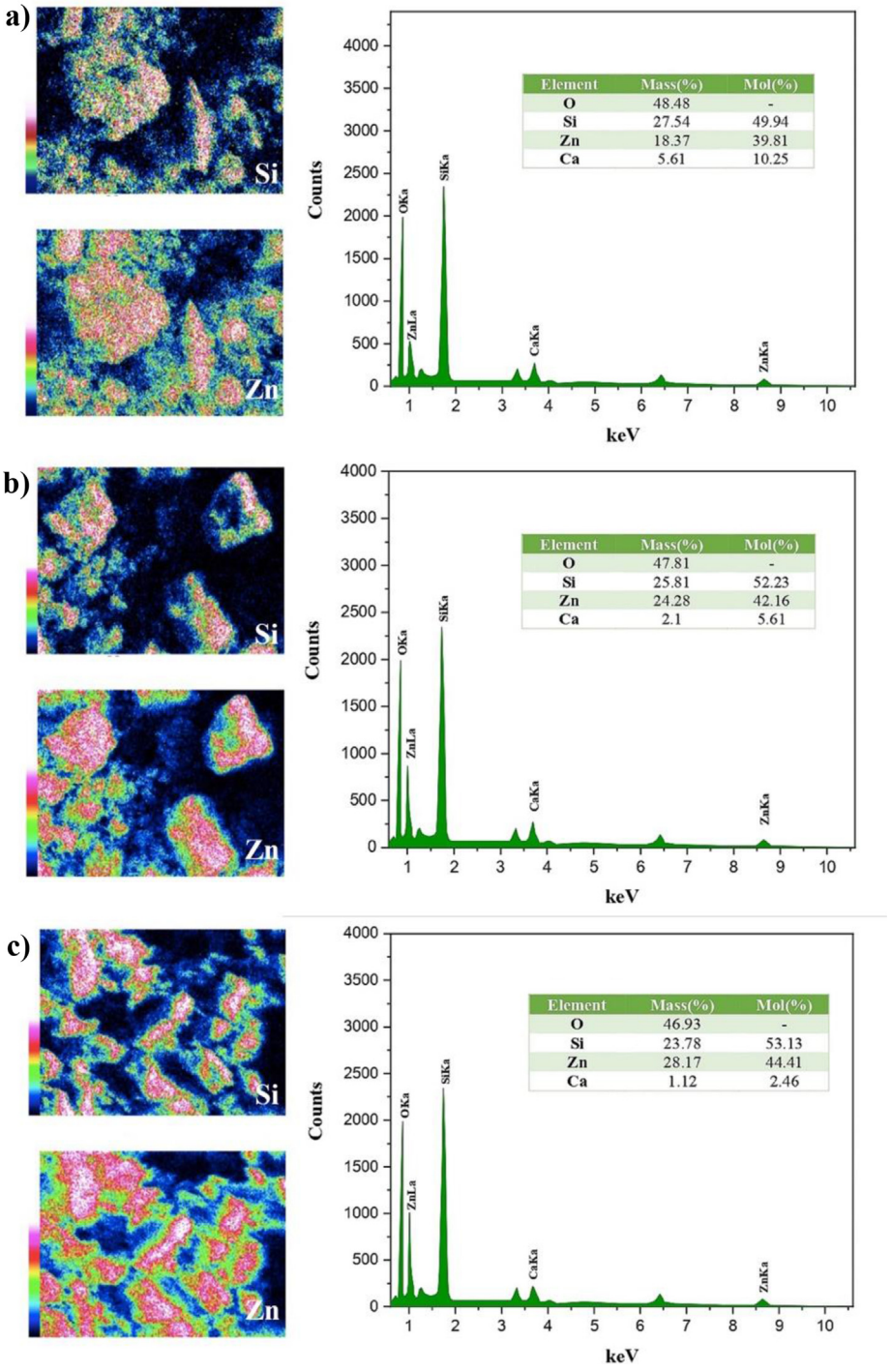

Fig. 9. EDX-Mapping anlysis of (a) ZnO/SiO_2-20, (b) ZnO/SiO_2-25, dan (c) ZnO/SiO_2-30.

The spherical morphology in catalytic materials presents several advantages that significantly enhance their performance. Firstly, the uniform and spherical structure contributes to an enhanced surface area, a crucial factor in catalysis [46] (presented in Table 4). This increasing surface area provides more active sites, thus increasing the efficiency of the catalyst in facilitating chemical reactions. Secondly, the uniform morphology of the spherical structure plays an important role in improving the mass transfer dynamics [47]. This results in better diffusion of reactants to active sites and efficient removal of products from the catalyst surface, ultimately leading to improved catalytic performance, conversion, and selectivity. Thirdly, the consistent distribution of active sites across the catalyst surface, ensured by the uniformity of spherical crystals, promotes uniform catalytic activity and selectivity [46]. Its characteristic allows for better control over reaction pathways, enhancing the overall effectiveness of the catalyst, especially in biodiesel conversion. Furthermore, the uniform and spherical structure contributes to the catalyst's resistance to deactivation. This well-defined morphology helps maintain the integrity of active sites during catalytic reactions, ensuring the stability of catalyst structure, increase the life time, and sustaining catalytic activity over time (will discuss in the next section).

The results obtained are similar to the morphology of the ZnO/SiO_2 composite synthesized from Merapi mountain ash [48]. The particle size distribution analysis using ImageJ software is shown in Fig. S1, which shows that catalyst particle size is below 10 μm. Also, the elemental composition of ZnO/SiO_2 was determined by EDX analysis as shown in Fig. 9. Elements such as O, Si, Zn, and Ca have significant peaks, confirming their presence in the composite structure. The peaks of Zn and Si elements are significant compared to the Ca element (present as an impurity). Based on EDX results, the mass percentage of Zn increases with increasing precursor amount. In addition, mapping analysis shows the distribution of Si and Zn elements in the sample. As shown, the elements are distributed on the catalyst surface as colored dots.

Based on the results of analysis using an FTIR spectrophotometer shown in Fig. 10, the biogenic SiO_2 produced shows the presence of −OH stretching and bending absorption, showing the presence of water bound to the biogenic SiO_2 sample from pineapple leaves. Additionally, typical SiO_2 absorption also appears at wave numbers 800-1000 cm^{-1} and 1300-1500 cm^{-1} which shows Si−O−Si symmetry and asymmetry respectively [49]. The ZnO sample shows very sharp absorption in the 400-500 cm^{-1} area. In all ZnO/SiO_2 catalyst samples, a Si−O−Si peak was observed at wave numbers ranging from 1029 to 1047 cm^{-1}. Furthermore, Zn−O absorption also appeared in the

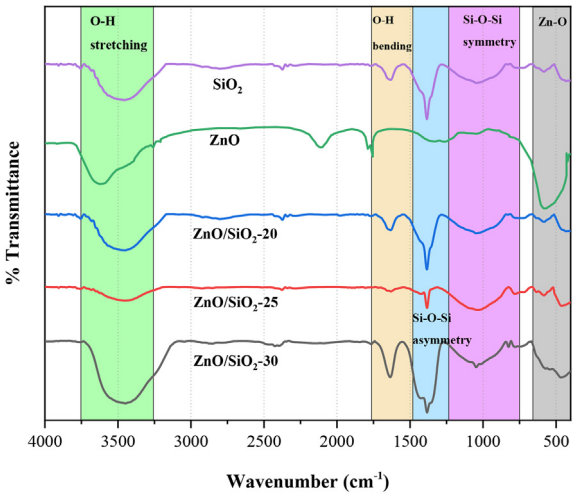

Fig. 10. FTIR spectra of ZnO/SiO_2.

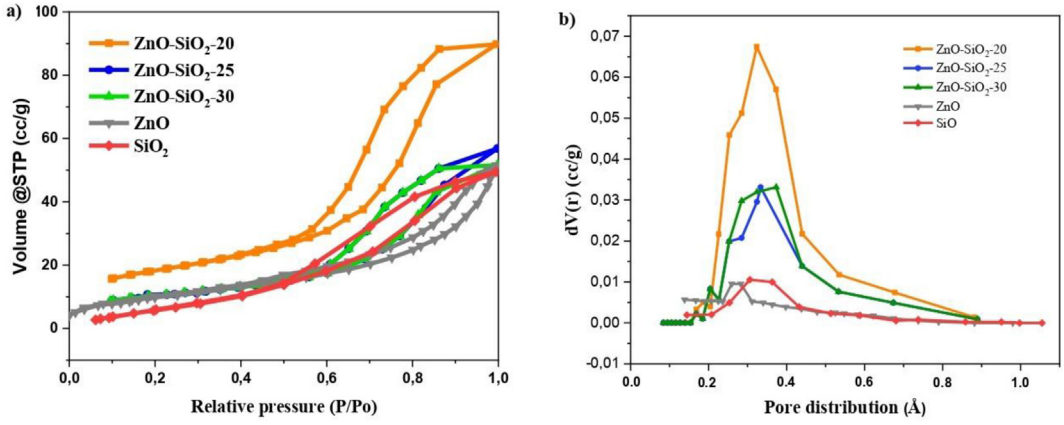

Fig. 11. a) N_2 adsorption and desorption isotherms (b) BJH pore distribution of ZnO/SiO_2.

fingerprint area 432-472 cm^{-1}. This is in line with the theory which shows functional groups in the ZnO/SiO_2 composite sample. This shows the presence of ZnO in the ZnO/SiO_2 catalyst. The bands about 3500 cm^{-1} and 1700 cm^{-1} belong to −OH stretching and bending respectively [49]. The presence of Zn−O adsorption on the sample will produce surface acid sites, where Zn^{2+} cations associate with PLA biogenic silica [50].

Textural properties analysis was carried out using SAA as shown in Fig. 11, it includes pore distribution using the BJH method and N_2 gas adsorption and desorption isotherms using the BET method. The obtained results indicate that the catalyst's surface area increases with increasing ZnO concentration, as Table 4 illustrates.

Based on the analysis results, the biogenic SiO_2 surface area in pineapple leaves is 59.12 m^2/g. The results obtained were lower than biogenic SiO2 from salacca fruit leaves [22]. Based on the IUPAC classification, the isotherms of catalysts are closed to Type V and the hysteresis loop is close to type H2, demonstrating that in microporous or mesoporous substances, modest gas−solid contact is possible [51]. In addition, both polar and non-polar molecules exhibit the type V adsorption isotherm. For instance, Type V isotherms are observed for water adsorption on hydrophobic microporous or mesoporous adsorbents [52]. This assumption is in line with the results of the BJH analysis which reported that pore volume was 0.19 cc/g with a pore distribution of 0.32 Å, which indicates the size of the pores produced by the catalyst, is micropores.

The ZnO/SiO_2 catalyst samples show that the greater the amount of ZnO, the larger the catalyst's surface area, as indicated in Table 4. The results obtained are in line with the trend produced by previous investigations which used biogenic silica from bamboo ash and salacca leaves ash [16,45]. The ZnO/SiO_2 catalyst made from the ash of salacca leaves has a surface area that is less than the resultant surface area [16]. The catalyst's pore distribution was also measured in addition to its surface area, and it consistently showed a range of 0.33−0.39 Å.

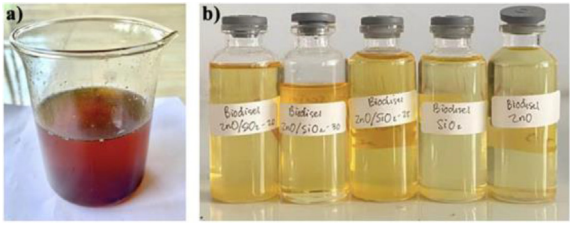

Fig. 12. The physical appearance of (a) WCO and (b) biodiesel.

3.2. Catalytic activity of ZnO/SiO_2

*Special description of the title. (dispensable)

Using a transesterification method to turn used WCO into biodiesel, the catalytic activity test of ZnO/SiO_2 samples from PLA was conducted. The percentage conversion of biodiesel was calculated quantitatively using the acid number of biodiesel produced from WCO conversion. The physical appearance of the WCO used and the results of its conversion into biodiesel using a ZnO/SiO_2 catalyst are shown in Fig. 12.

Fig. 13 shows the transesterification reaction using biogenic SiO_2 and ZnO catalyst produces a lower conversion percentage compared to using a bimetal catalyst with all variations in ZnO concentration. This shows that even without a ZnO catalyst, the biogenic SiO_2 support is also able to prepare active sites in catalytic reactions in the form of Lewis acids as previously reported [53]. Moreover, the presence of ZnO on catalyst surface signifies an enhanced capacity to generate Lewis acid sites, crucial for the

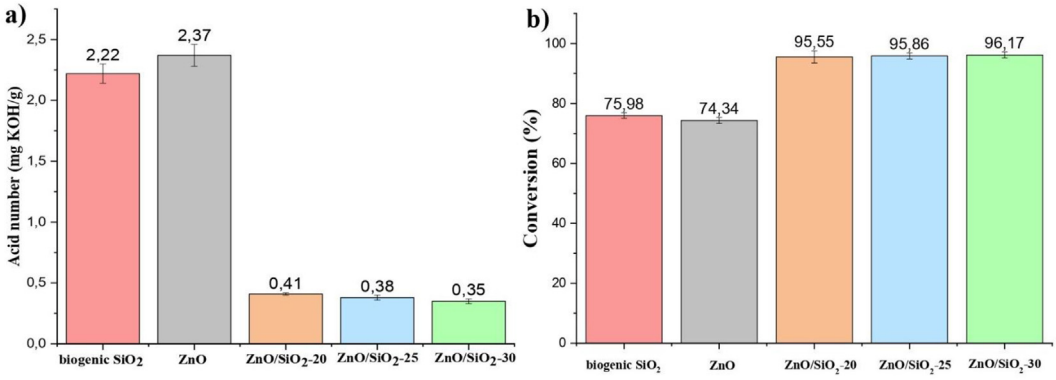

Fig. 13. (a) Acid number and (b) conversion biodiesel by transesterification reaction (methanol oil reaction 3:1) using 1 g ZnO/SiO_2 at 60 °C for 6 h.

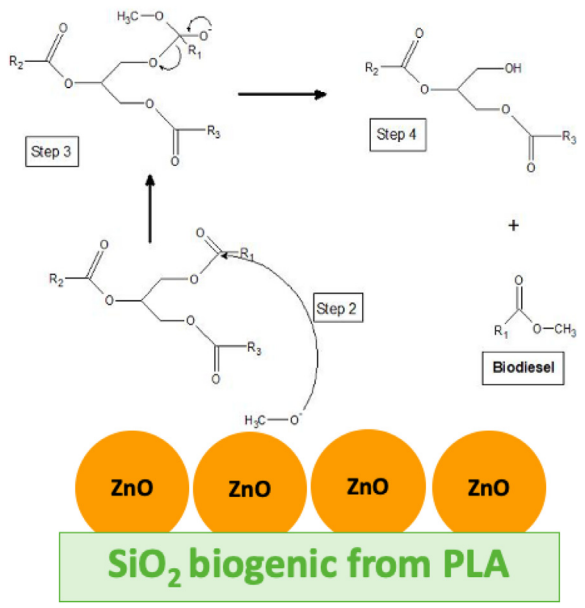

Fig. 14. The possible mechanism for WCO conversion to biodiesel using ZnO/SiO_2 catalyst.

adsorption process of used cooking oil. This is achieved through Lewis acid–base interactions, particularly with π bonds in the double bonds of carbonyl functional groups [16].

The results obtained show that the influence of ZnO content in ZnO/SiO_2 composites is quite significant on the percent conversion of biodiesel. It can be inferred that surface acidity has a greater influence on the percent conversion because the ZnO content is consistent with the specified surface acidity and the catalyst dose is correlated with the catalyst's specific surface area (Table 4) [16]. Apart from that, it can also be associated with the peak of the XRD diffractogram (Fig. 7) which shows the presence of wurtzite and quartz phases which are supported by the FTIR absorption band (Fig. 10), where there is absorption at wave numbers 1607 cm^{-1} and 1465 cm^{-1} corresponding to the Lewis acid and Brønsted acid sites, respectively [16]. The methyl shift indicates catalytic reaction on the catalyst surface, proton migration, and bond rear-

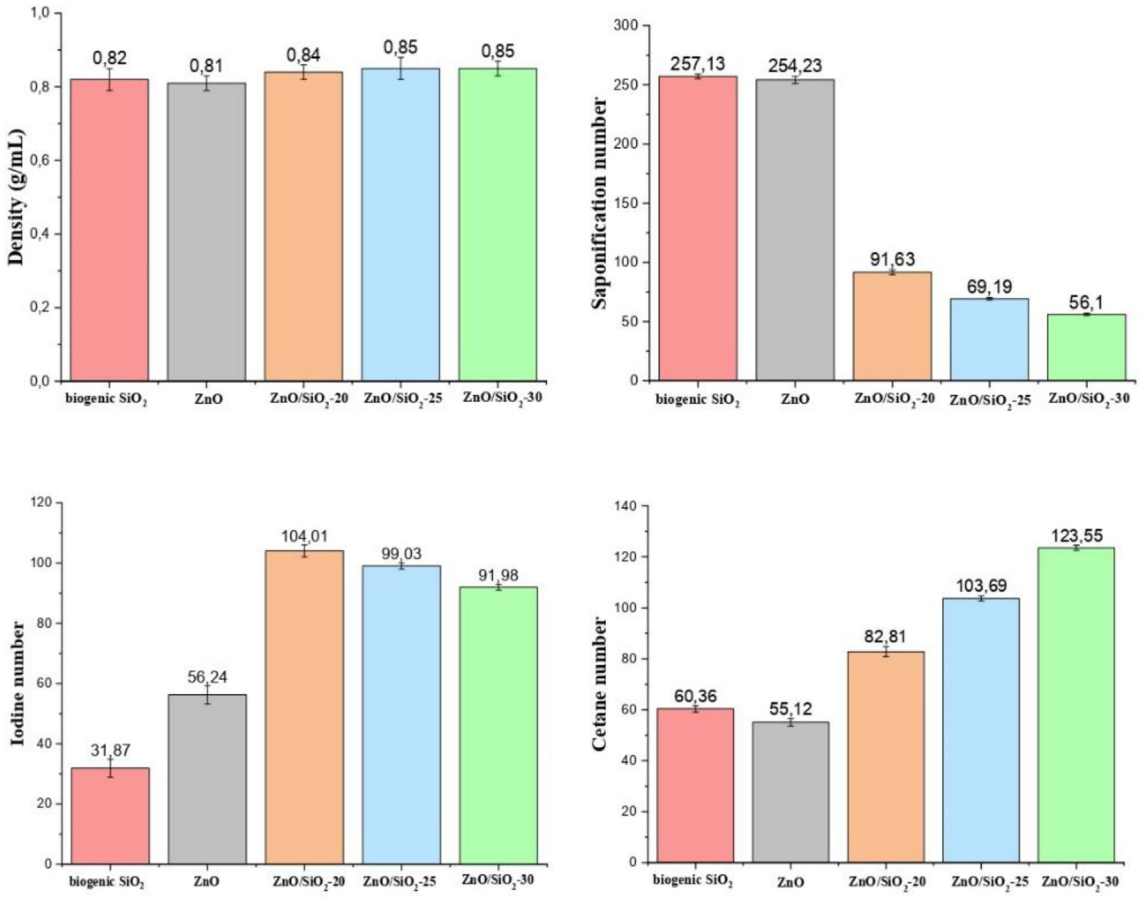

Fig. 15. The results of quantitative analysis of biodiesel quality by transesterification reaction (methanol oil reaction 3:1) using 1 g ZnO/SiO_2 at 60 °C for 6 h.

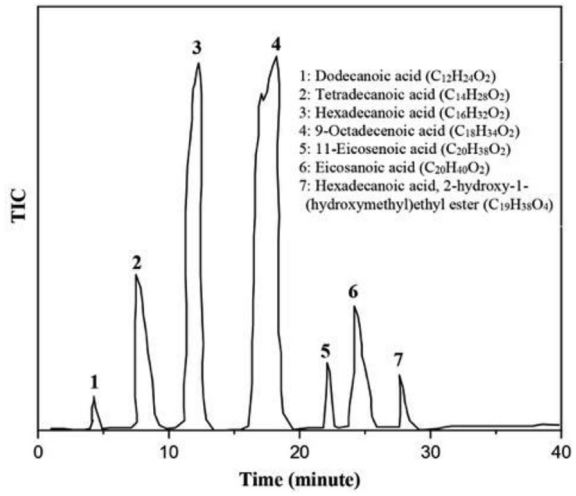

Fig. 16. GC–MS analysis profile of produced biodiesel.

rangement between reactants and Zn surface followed by desorption of methyl ester and alcohol/glycerol as products (will be discussed in the reusability test section in Fig. 20). Therefore, the possible mechanism shown in Fig. 14. The highest percentage conversion was 96.17 % using the ZnO/SiO_2-30 catalyst, which can be attributed to the high amount of ZnO in the sample (Table 2) with a very sharp wurtzite phase peak with the greatest intensity in the XRD diffractogram (Fig. 7).

Additionally, quantitative analysis was also carried out in the form of density, saponification number, iodine number, and cetane number of biodiesel as shown in Fig. 15. The outcomes demonstrated that the biodiesel's quality complies with SNI 7182:2015.

Biodiesel with the highest conversion (using ZnO/SiO_2-30) was then subjected to qualitative analysis to determine the type of hydrocarbon contained in the sample, as shown in Fig. 16. The GC–MS diffractogram confirmed the presence of methyl ester in the synthesized biodiesel with a C_{12}–C_{20} carbon chain. The dominant components observed were methyl esters of hexadecanoic acid, octadecanoic acid, tetradecanoic acid, and eicosanoic acid. Besides, dodecanoic acid and hexadecanoic acid are minor components of methyl ester. The composition is similar to the previous study which used rice bran oil as feedstock and biogenic silica as a ZnO catalyst support [16]. The composition obtained is also similar to the previous study which used WCO as a feedstock catalyzed by CaO [54]. Therefore, biodiesel resulting from WCO transesterification

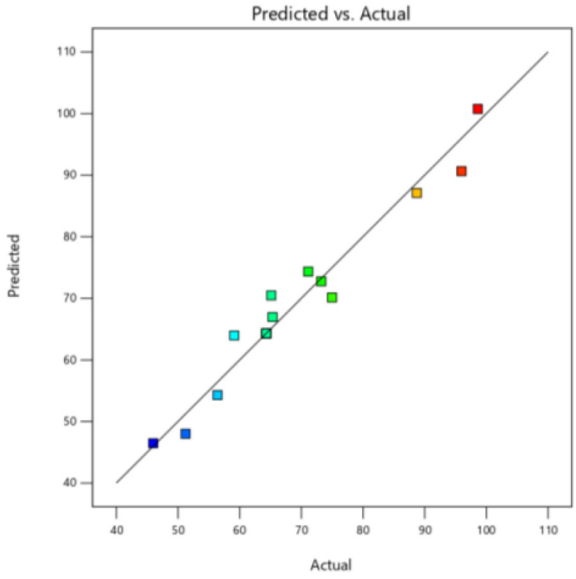

Fig. 17. Plot of actual and predicted yield.

Table 5. The yield value at the varied conditions.

Run	Factor 1 A:Catalyst dose (g)	Factor 2 B:Reaction time (hours)	Factor 3 C:Temperature (°C)	Response Yield %
1	0.5	4	57.5	56.41
2	1.75	6	57.5	84.31
3	0.5	6	65	60.98
4	1.75	6	57.5	84.33
5	1.75	6	57.5	84.29
6	3	4	57.5	56.12
7	1.75	8	50	65.8
8	3	6	57.5	98.62
9	1.75	4	65	61.23
10	3	6	65	88.72
11	1.75	8	65	73.24
12	3	6	50	95.98
13	0.5	6	50	84.98
14	1.75	6	57.5	84.35
15	1.75	4	50	45.98
16	0.5	8	57.5	80.15

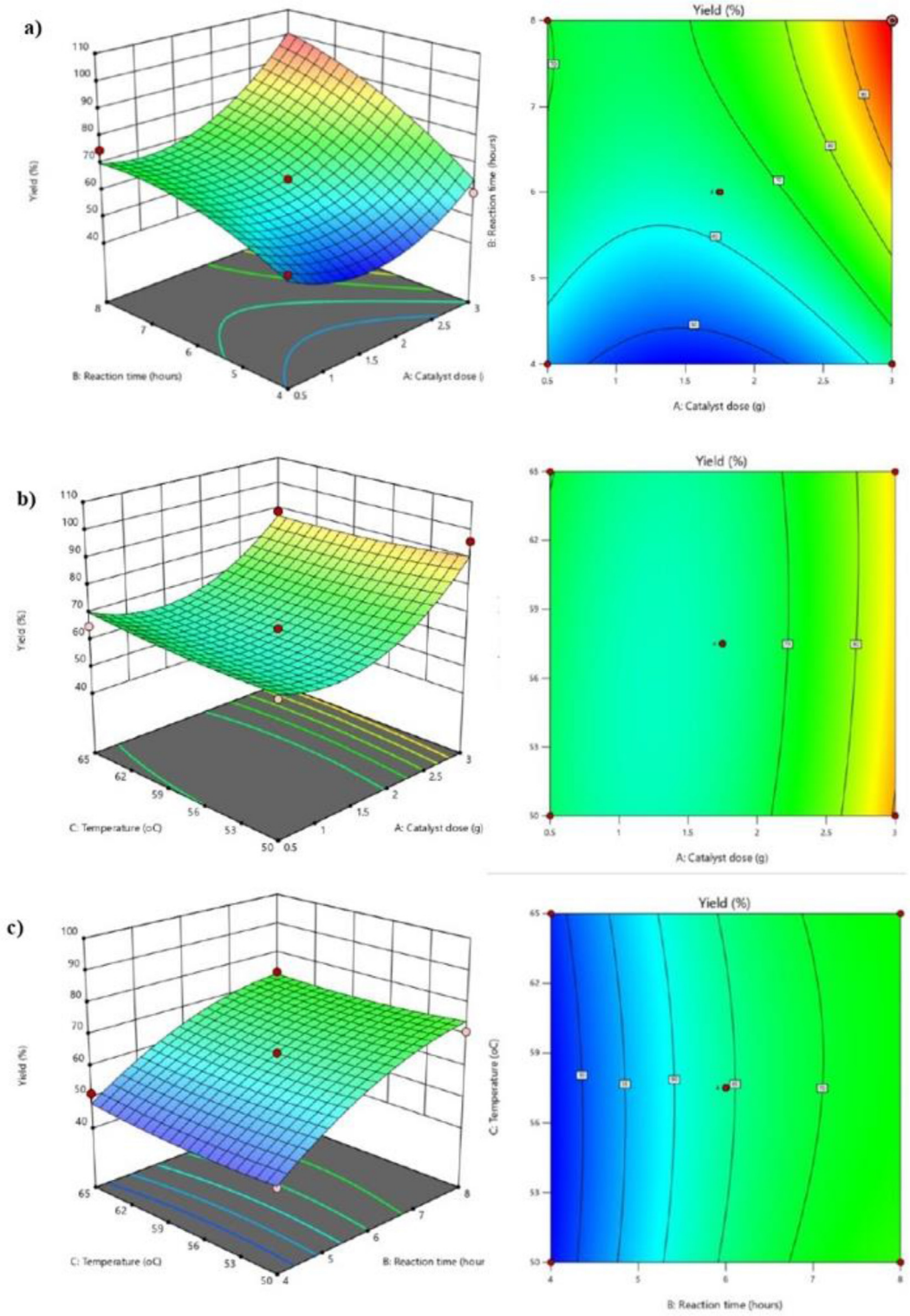

Fig. 18. Response surface interaction and contour plots showing the effect of (a) catalyst dose and reaction time, (b) catalyst dose and temperature, (c) reaction time and temperature.

catalyzed by ZnO supported by biogenic SiO_2 PLA fulfills SNI and ASTM standards.

Optimization of catalytic activity was carried out based on CCD using ZnO/SiO_2-30 composite. Table 5 shows the yields under varying conditions with the results of the analysis of variance (ANOVA) of the response surface model shown in Table S1. The statistical parameters show that the regression

model is significant at the 95 % confidence level with the predictability of the model. The coefficient of determination or R^2 of 0.9573 indicates that the model can be used as a response predictor. In addition, the relatively high coefficient of variation value indicates the high reliability of the experiment.

The plot in Fig. 17 was created to ensure the adequacy of the proposed regression model. The obtained R^2 is 0.973 which represents the fitness of the model. Furthermore, response surface interaction and contour plots in Fig. 18 shows that higher yields can be achieved at time reaction, catalyst dose and certain temperature. At runs 1 and 6 (Table 5) with the same temperature and reaction time, the higher catalyst dose produces a lower yield. This can be attributed to increasing the amount of catalyst causing an increase in the viscosity of the reaction medium. As a consequence, the mass transfer rate of reactants to the catalyst surface decreases, resulting in lower conversion [55]. In addition, high catalyst loads can also cause particle aggregation, reducing surface area and blocking active sites, thereby further reducing reactivity [56]. This same behavior was also observed with previous research which also used natural ingredients in the form of waste cupuaçu seeds as the raw catalyst [57]. Apart from that, it can be seen that the longer reaction time, the biodiesel yield also increases. However, in runs 8 and 11 (Table 5) with a longer reaction time of 8 h, there was a decrease in biodiesel yield, which was thought to be due to the different number of catalysts, thus the optimal time was set at 6 h. The similar trend was also observed in previous studies that used electrolytic paste of spent batteries as a catalyst [58]. The plot and model conclude that the optimum conditions for producing biodiesel use a ZnO/SiO_2 catalyst of 3 g and a temperature of 57.5 °C.

3.3. Kinetic study

The transesterification reaction's rate can be assessed using kinetic parameters. The pseudo-first-order (PFO) kinetic model was utilized to explore the kinetic behaviours of biodiesel synthesis from WCO using ZnO/SiO_2 from PLA catalyst. For simplify, it is assumed that the oil and methanol reactants in a one-step with reversible [59]. The PFO model is expressed as follows in a simplified equation (2).

$$Ln(1-x) = -kt \quad (2)$$

Where k and x described reaction rate constant (1/min) and the biodiesel yield at time t. Fig. 19 illustrates that the PFO kinetic model fits to the experimental data because the R^2 value is greater than 0.95 carried out at a temperature of 57.5 °C. The reaction rate constant obtained is 0.3213 min^{-1} which is greater than the rate constant obtained in previous study [59,60]. This is expected to be because the reaction time used in this study was longer than in previous studies. However, the process carried out in this study is quite effective because it is carried out at low temperatures, is a simple method and uses natural materials as a catalyst source, as well as non-edible oil as biodiesel feedstock.

3.4. Catalyst reusability

Catalyst reuse is a crucial consideration for practical applications, and it is assessed by monitoring changes in yield over successive reaction cycles [61]. The catalyst was recycled by drying it at 100 °C and

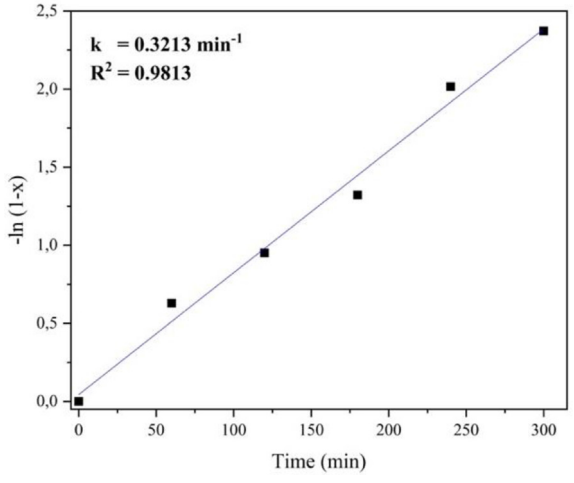

Fig. 19. PFO kinetic plot for determination of k values at 57.5 °C.

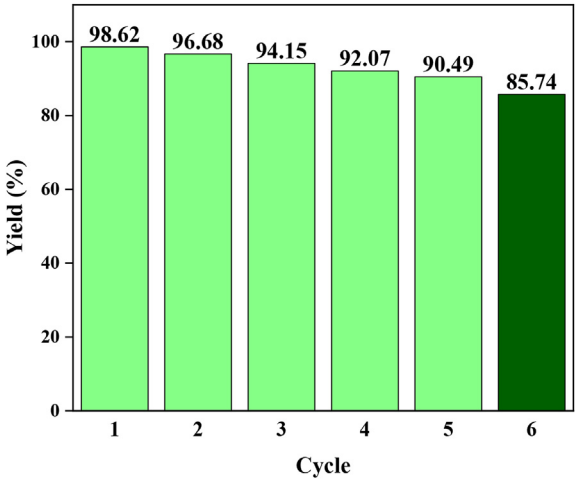

Fig. 20. Reusability test of catalyst using 3 g ZnO/SiO₂-30, reaction time 6 h at 57.5 °C.

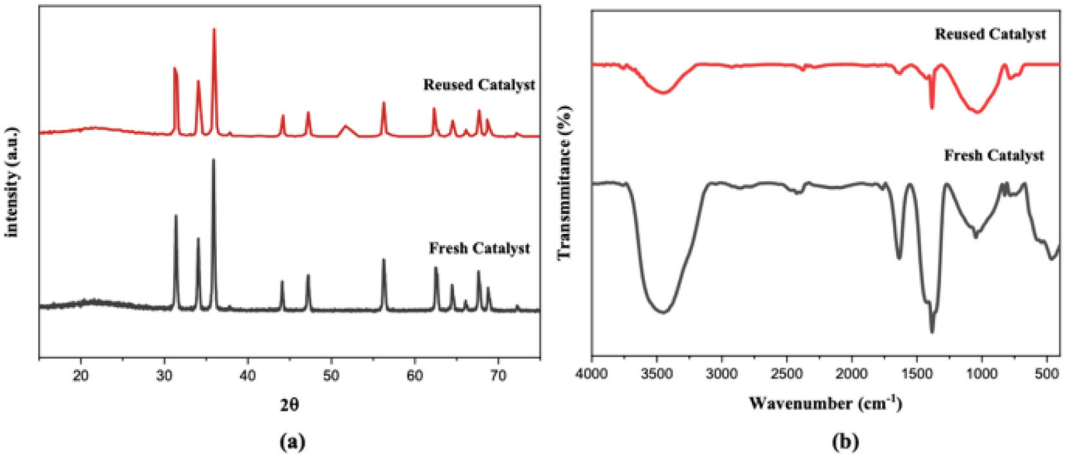

Fig. 21. (a) XRD and (b) FTIR pattern of reused ZnO/SiO_2 catalyst.

washing it in ethanol and water. Fig. 20 shows that the catalyst exhibits good reusability up to the fifth cycle, with the conversion percentage remaining at a lowered value of no more than 15 % of the fresh catalyst. However, the sixth cycle showed a considerable decline in results. The loss of catalytic characteristics in the composite hinders its ability to facilitate surface reactions, as demonstrated.

Furthermore, to examine the stability of the catalyst during the biodiesel production process for up to sixth cycles, investigations were carried out using XRD and FTIR for fresh and reused catalysts, as shown in Fig. 21. After using the catalyst for biodiesel conversion, it was observed in the XRD diffractogram (Fig. 21a), a new peak appeared at 54.84° which indicated the leaching process [57,62]. In addition, it can be observed that there is a decrease in peak intensity at 56.29° and 62.57° which is as dense as ZnO wurtzite. Leaching was also observed when the catalyst was analyzed by FTIR (Fig. 21b), the loss of −OH and Zn−O absorption at wavenumbers 1600 cm^{-1} and 435 cm^{-1}. This is thought to be caused by pore filling and surface poisoning due to triglycerides and glycerol which reduce the active sites on the catalyst surface [55]. Therefore, biodiesel generation has caused small changes to the crystal phase and functional groups of the catalyst, but no changes have occurred to the overall catalyst structure.

Table 6 compares the recyclability of various catalyst in generating biodiesel. Based on previous investigations, the ZnO/SiO_2 catalyst from PLA used in this study showed extraordinary stability compared with heterogeneous catalysts using pure SiO_2 [30]. However, the efficiency of the heterogeneous catalyst in this study is lower than previous research which used date palm seeds as the raw material for the AC@ZnO/NiO catalyst which can be used for up to 7 cycles with a biodiesel yield of 97.81 % using an ultrasonic reactor [15]. This is expected because the biodiesel conversion process only uses conventional methods so it is very necessary to develop the use of more advanced methods in order to increase the efficiency of catalyst performance.

Based on Tables 6 and it can be seen that the performance of PLA as a catalyst produces extraordinary yields with a low number cycles. However, after PLA was modified with ZnO (present study) the number of catalyst reuse cycles increased. Furthermore, performance of catalysts based on biogenic silica from PLA is almost similiar as other studies that use pure materials. When compared to using MCM-41 as a catalyst support, the biogenic

Table 6. Comparing the efficiency of biodiesel conversion using various heterogenous catalyst.

Catalyst	Conditions	BY (%)	Cycle no.	Ref.
AC@ZnO/NiO	CD: 2.41 wt%; t: 36.62 min; T: 65 °C; MOR: 11.24:1	97.81	7	[15]
$CoFe_2O_4$@GO	CD: 5.22 wt%; t: 55.75 min; T: 64.75 °C; MOR: 16.05:1	98.17	5	[60]
$MnFe_2O_4$@biochar	CD: 1.75 wt%; t: 56.12 min; MOR: 11.35:1	97.26	7	[34]
UiO-66-NH_2/ZnO/TiO_2	CD: 2 wt%; T: 60 °C; MOR: 9.8:1	98.70	7	[59]
Fe_3O_4/SiO_2@ZnO	CD: 2.67 wt%; t: 30.13 min; MOR: 9.90:1	97.23	7	[31]
CaO−Zr/MCM-41	CD: 5 wt%; t: 6 h; T: 65 °C; MOR: 9:1	88.50	5	[63]
ZnO/SiO_2 from salacca leaves	CD: 5 g; t: 3 h; T: 65 °C; MOR: 3:1	98.44	5	[16]
PLA	CD: 4 wt%; t: 30 min; T: 60 °C; MOR: 1:40	98.92	3	[27]
ZnO/SiO_2 from PLA	CD: 3 g; t: 6 h; T: 57.5 °C; MOR: 3:1	98.62	6	present

CD: catalyst dosage; t: reaction time; T: temperature; MOR: methanol oil ratio; BY: Biodiesel yield.

silica produced in this study is more effective because it uses a smaller catalyst dosage with a greater biodiesel yield. Furthermore, this research is more cost effective because it uses agricultural waste as catalyst raw material and household waste in the form of WCO as biodiesel feedstocks. Thus, the results obtained are very beneficial for a sustainable economy.

4. Conclusion

In conclusion, this study showed that ZnO/SiO_2 was successfully prepared entirely using silica derived from PLA by examining the influence of the amount of ZnO. The data obtained showed that all of the ZnO/SiO_2 composite samples possessed characteristics suitable for use as catalyst. The ZnO/SiO_2 catalyst samples exhibited a hexagonal wurtzite polycrystalline structure, with an average crystal size of 31.83–34.15 nm, and a uniform morphology of the crystals making up catalyst with a ball-like shape. The surface area of the samples produced increased as the amount of ZnO increased from 88.97 m^2/g to 93.41 m^2/g. The sample showed efficient catalytic activity for conversion of biodiesel from WCO with the best conversion using a ZnO/SiO_2-30 catalyst of 96.17 %. Biodiesel produced was a C_{12}–C_{20} carbon chain with the optimum reaction conditions used 3 g of ZnO/SiO_2-30, reaction time 6 h at 57.5 °C and WCO to methanol ratio of 3:1 with a yield of 98.62 %. The resulting catalyst has extraordinary durability up to sixth cycles. This showed that the material has the potential to be developed for biodiesel conversion at low cost and sustainable resources for future. Furthermore, it is promised that in the future we can obtain much better results by utilizing other raw materials, and exploring new catalytic supports that are more environmentally friendly.

Acknowledgments

The authors express profound gratitude to Direktorat Jenderal Pendidikan Tinggi, Riset, dan Teknologi through Direktorat Pembelajaran dan Kemahasiswaan for providing study grants to the Program Kreativitas Mahasiswa-Riset Eksakta (PKM-RE) scheme, as well as to Universitas Negeri Makassar for support in carrying out this study.

Appendix.

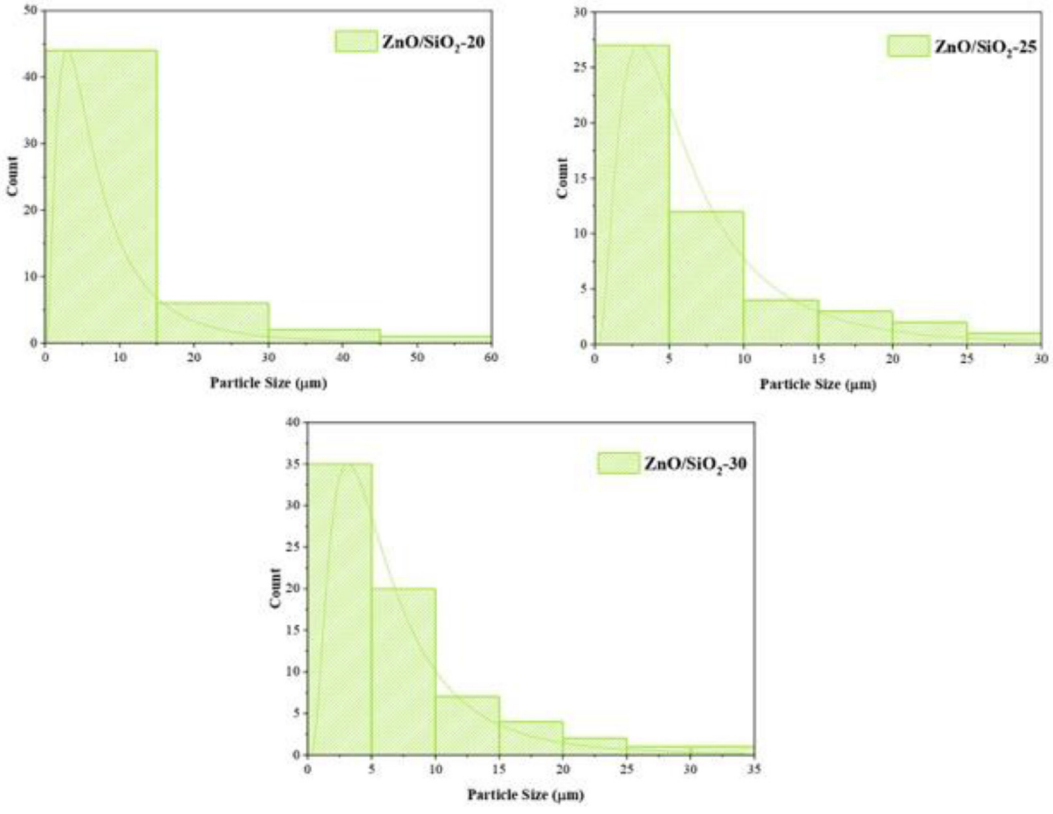

Fig. S1. Analysis of particle size distribution of ZnO/SiO_2

Table S1. ANOVA results for full-factor analysis

Source	Sum of Squares	Degrees of Freedon	Mean Square	F-value	p-value	
Model	3130.78	9	347.86	14.94	0.0019	significant
A-Catalyst dose	811.84	1	811.84	34.87	0.0010	
B-Reaction time	1383.91	1	1383.91	59.44	0.0002	
C-Temperature	0.0015	1	0.0015	0.0001	0.9938	
AB	109.52	1	109.52	4.70	0.0732	
AC	12.39	1	12.39	0.5321	0.4932	
BC	2.45	1	2.45	0.1052	0.7567	
A^2	695.25	1	695.25	29.86	0.0016	
B^2	108.73	1	108.73	4.67	0.0740	
C^2	6.70	1	6.70	0.2875	0.6111	
Residual	139.70	6	23.28			
Lack of Fit	139.70	3	46.57	1.597E+05	<0.0001	not significant
Pure Error	0.0009	3	0.0003			
Cor Total	3270.48	15				

References

[1] F. Ullah, L. Dong, A. Bano, Q. Peng, J. Huang, Current advances in catalysis toward sustainable biodiesel production, J Energy Inst 89 (2016) 282–292, https://doi.org/10.1016/j.joei.2015.01.018.

[2] M. Al Muttaqii, M. Amin, E. Prasetyo, R. Alviany, L. Marlinda, Production of biodiesel over ZnO-TiO2bifunctional oxide catalyst supported on natural zeolite, IOP Conf Ser Earth Environ Sci 926 (2021) 1754–1762, https://doi.org/10.1088/1755-1315/926/1/012083.

[3] T.C. Venkateswarulu, I. Mikkili, K. Srirama, B. Md Nazneen, J.B. Dulla, V.N. Alugunulla, S. Vivekananda, A. Peele, P. Bangaraiah, Biodiesel production from chicken feather meal and its performance analysis on diesel engine, Karbala Int. J. Mod. Sci. 6 (2020) 1–6, https://doi.org/10.33640/2405-609X.1205.

[4] I. Istadi, S.A. Prasetyo, T.S. Nugroho, Characterization of K_2O/CaO-ZnO catalyst for transesterification of soybean oil to biodiesel, Procedia Environ. Sci. 23 (2015) 394–399, https://doi.org/10.1016/j.proenv.2015.01.056.

[5] M.G. Basyouny, M.R. Abukhadra, K. Alkhaledi, A.M. El-Sherbeeny, M.A. El-Meligy, A.T.A. Soliman, M. Luqman, Insight into the catalytic transformation of the waste products of some edible oils (corn oil and palm oil) into biodiesel using MgO/clinoptilolite green nanocomposite, Mol Catal 500 (2021) 111340–111352, https://doi.org/10.1016/j.mcat.2020.111340.

[6] I. Ambat, V. Srivastava, S. Iftekhar, E. Haapaniemi, M. Sillanpää, Effect of different co-solvents on biodiesel production from various low-cost feedstocks using Sr–Al double oxides, Renew Energy 146 (2020) 2158–2169, https://doi.org/10.1016/j.renene.2019.08.061.

[7] R. Naveenkumar, G. Baskar, Process optimization, green chemistry balance and technoeconomic analysis of biodiesel production from castor oil using heterogeneous nanocatalyst, Bioresour Technol 320 (2021) 124347, https://doi.org/10.1016/j.biortech.2020.124347.

[8] C. Adhikesavan, D. Ganesh, V. Charles Augustin, Effect of quality of waste cooking oil on the properties of biodiesel, engine performance and emissions, Clean. Chem. Eng. 4 (2022) 100070, https://doi.org/10.1016/j.clce.2022.100070.

[9] Y. Zhang, L. Duan, H. Esmaeili, A review on biodiesel production using various heterogeneous nanocatalysts: operation mechanisms and performances, Biomass Bioenergy 158 (2022) 106356, https://doi.org/10.1016/j.biombioe.2022.106356.

[10] H. Rasouli, H. Esmaeili, Characterization of MgO nanocatalyst to produce biodiesel from goat fat using transesterification process, Biotech 39 (2019) 429, https://doi.org/10.1007/s13205-019-1963-6.

[11] S.N. Gebremariam, T. Hvoslef-Eide, M.T. Terfa, J.M. Marchetti, Techno-economic performance of different technological based bio-refineries for biofuel production, Energies 12 (2019) 3916, https://doi.org/10.3390/en12203916.

[12] H. Esmaeili, A critical review on the economic aspects and life cycle assessment of biodiesel production using heterogeneous nanocatalysts, Fuel Process Technol 230 (2022) 107224, https://doi.org/10.1016/j.fuproc.2022.107224.

[13] K. Seffati, H. Esmaeili, B. Honarvar, N. Esfandiari, AC/$CuFe_2O_4$@CaO as a novel nanocatalyst to produce biodiesel from chicken fat, Renew Energy 147 (2020) 25–34, https://doi.org/10.1016/j.renene.2019.08.105.

[14] A.S. Yusuff, J.O. Owolabi, Synthesis and characterization of alumina supported coconut chaff catalyst for biodiesel production from waste frying oil, South Afr J Chem Eng 30 (2019) 42–49, https://doi.org/10.1016/j.sajce.2019.09.001.

[15] B. Maleki, Y. Kalanakoppal Venkatesh, S. Siamak Ashraf Talesh, H. Esmaeili, S. Mohan, G.R. Balakrishna, A novel biomass derived activated carbon mediated AC@ZnO/NiO bifunctional nanocatalyst to produce high-quality biodiesel from dairy industry waste oil: CI engine performance and emission, Chem. Eng. J. 467 (2023) 143399, https://doi.org/10.1016/j.cej.2023.143399.

[16] I. Fatimah, G. Purwiandono, I. Sahroni, S. Sagadevan, W. Chun-Oh, S.A.I.S.M. Ghazali, R. an Doong, Recyclable catalyst of ZnO/SiO_2 prepared from salacca leaves ash for sustainable biodiesel conversion, South Afr J Chem Eng 40 (2022) 134–143, https://doi.org/10.1016/j.sajce.2022.02.008.

[17] F.S. Zainulabdeen, J.O. Dahloos, A.F. Atwan, N.K. Kasim, Optical measurement and performance prediction of solar PV system in Al-khidhir zone/Iraq, Karbala Int. J. Mod. Sci. 8 (2022) 126–133, https://doi.org/10.33640/2405-609X.3216.

[18] S. Einloft, T. Magalhães, A. Donato, J. Lima, R. Ligabue, Biodiesel from rice bran oil: transesterification by tin compounds, Energy Fuels 22 (2008) 671–674, https://doi.org/10.1021/ef700510a.

[19] M.A. Zahed, M. Revayati, N. Shahcheraghi, F. Maghsoudi, Y. Tabari, Modeling and optimization of biodiesel synthesis using TiO_2–ZnO nanocatalyst and characteristics of biodiesel made from waste sunflower oil, Curr. Res. Green Sustain. Chem. 4 (2021) 100223, https://doi.org/10.1016/j.crgsc.2021.100223.

[20] P. Zhang, X. Chen, Y. Leng, Y. Dong, P. Jiang, M. Fan, Biodiesel production from palm oil and methanol via zeolite derived catalyst as a phase boundary catalyst: an optimization study by using response surface methodology, Fuel 272 (2020) 117680, https://doi.org/10.1016/j.fuel.2020.117680.

[21] Shobhana-Gnanaserkhar, N. Asikin-Mijan, G. AbdulKareem-Alsultan, Sivasangar-Seenivasagam, S.M. Izham, Y.H. Taufiq-Yap, Biodiesel production via simultaneous esterification and transesterification of chicken fat oil by mesoporous sulfated Ce supported activated carbon, Biomass Bioenergy 141 (2020) 105714, https://doi.org/10.1016/j.biombioe.2020.105714.

[22] Y. Zhang, S. Niu, C. Lu, Z. Gong, X. Hu, Catalytic performance of $NaAlO_2/\gamma$-Al_2O_3 as heterogeneous nanocatalyst for biodiesel production: optimization using response surface methodology, Energy Convers Manag 203 (2020) 112263, https://doi.org/10.1016/j.enconman.2019.112263.
[23] I.M.R. Fattah, M.Y. Noraini, M. Mofijur, A.S. Silitonga, I.A. Badruddin, T.M.Y. Khan, H.C. Ong, T.M.I. Mahlia, Lipid extraction maximization and enzymatic synthesis of biodiesel from microalgae, Appl Sci 10 (2020) 6103, https://doi.org/10.3390/app10176103.
[24] D. Shrestha, T. Nayaju, M.R. Kandel, R.R. Pradhananga, C.H. Park, C.S. Kim, Rice husk-derived mesoporous biogenic silica nanoparticles for gravity chromatography, Heliyon 9 (2023) e15142, https://doi.org/10.1016/j.heliyon.2023.e15142.
[25] I. Fatimah, N.I. Prakoso, I. Sahroni, M.M. Musawwa, Y.L. Sim, F. Kooli, O. Muraza, Physicochemical characteristics and photocatalytic performance of TiO_2/SiO_2 catalyst synthesized using biogenic silica from bamboo leaves, Heliyon 5 (2019) 02766, https://doi.org/10.1016/j.heliyon.2019.e02766.
[26] H. Heryani, N.R. Yanti, Potentials of biomass waste sources for heterogeneous catalyst production, IOP Conf Ser Earth Environ Sci 472 (2020) 012035, https://doi.org/10.1088/1755-1315/472/1/012035.
[27] S. de S. Barros, W.A.G. Pessoa Junior, I.S.C. Sá, M.L. Takeno, F.X. Nobre, W. Pinheiro, L. Manzato, S. Iglauer, F.A. de Freitas, Pineapple (*Ananás comosus*) leaves ash as a solid base catalyst for biodiesel synthesis, Bioresour Technol 312 (2020) 123569, https://doi.org/10.1016/j.biortech.2020.123569.
[28] H. Heryani, A. Ghofur, N. Chairunnisa, Esterification of acetin production from by-products of biodiesel industry using heterogeneous catalysts based on wetland commodities, Pertanika J. Sci. Technol. 30 (2022) 1861–1882, https://doi.org/10.47836/pjst.30.3.06.
[29] F. Kesserwan, M.N. Ahmad, M. Khalil, H. El-Rassy, Hybrid CaO/Al_2O_3 aerogel as heterogeneous catalyst for biodiesel production, Chem. Eng. J. 385 (2020) 123834, https://doi.org/10.1016/j.cej.2019.123834.
[30] N.S. Lani, N. Ngadi, I.M. Inuwa, New route for the synthesis of silica-supported calcium oxide catalyst in biodiesel production, Renew Energy 156 (2020) 1266–1277, https://doi.org/10.1016/j.renene.2019.10.132.
[31] B. Maleki, H. Esmaeili, Application of Fe_3O_4/SiO_2@ZnO magnetic composites as a recyclable heterogeneous nanocatalyst for biodiesel production from waste cooking oil: response surface methodology, Ceram Int 49 (2023) 11452–11463, https://doi.org/10.1016/j.ceramint.2022.11.344.
[32] B. Maleki, H. Esmaeili, Ultrasound-assisted conversion of waste frying oil into biodiesel using Al-doped ZnO nanocatalyst: box-Behnken design-based optimization, Renew Energy 209 (2023) 10–26, https://doi.org/10.1016/j.renene.2023.03.119.
[33] B. Maleki, B. Singh, H. Eamaeili, Y.K. Venkatesh, S.S.A. Talesh, S. Seetharaman, Transesterification of waste cooking oil to biodiesel by walnut shell/sawdust as a novel, low-cost and green heterogeneous catalyst: optimization via RSM and ANN, Ind Crops Prod 193 (2023) 116261, https://doi.org/10.1016/j.indcrop.2023.116261.
[34] B. Maleki, Y. Kalanakoppal Venkatesh, B. Muthusamy, H. Esmaeili, A cleaner approach towards magnetically assisted-electrolysis of biodiesel production using novel $MnFe_2O_4$@ sawdust derived biochar nanocatalyst and its performance on a CI engine, Energy Convers Manag 299 (2024) 117829, https://doi.org/10.1016/j.enconman.2023.117829.
[35] D.Y.C. Leung, X. Wu, M.K.H. Leung, A review on biodiesel production using catalyzed transesterification, Appl Energy 87 (2010) 1083–1095, https://doi.org/10.1016/j.apenergy.2009.10.006.
[36] J. Toledo Arana, J.J. Torres, D.F. Acevedo, C.O. Illanes, N.A. Ochoa, C.L. Pagliero, One-step synthesis of CaO-ZnO efficient catalyst for biodiesel production, Int J Chem Eng 2019 (2019) 1–8, https://doi.org/10.1155/2019/1806017.
[37] Z.A. Najm, M.A. Atiya, A.K. Hassan, Biogenesis Synthesis of ZnO NPs: its adsorption and photocatalytic activity for removal of acid black 210 dye, Karbala Int. J. Mod. Sci. 9 (2023) 514–528, https://doi.org/10.33640/2405-609X.3315.
[38] K. Kusdianto, W. Widiyastuti, M. Shimada, L. Qomariyah, S. Winardi, Fabrication of ZnO-SiO_2 nanocomposite materials prepared by a spray pyrolysis for the photocatalytic activity under UV and sunlight irradiations, IOP Conf Ser Mater Sci Eng 778 (2020) 012105, https://doi.org/10.1088/1757-899X/778/1/012105.
[39] S. Raha, M. Ahmaruzzaman, ZnO nanostructured materials and their potential applications: progress, challenges and perspectives, Nanoscale Adv 4 (2022) 1868–1925, https://doi.org/10.1039/D1NA00880C.
[40] S.E. Putri, N. Herawati, A. Fudhail, D.E. Pratiwi, S. Side, A. Rahman, S.S. Desa, N. Ahmad, S. Junaedi, A. Surleva, Biosynthesis of copper nanoparticles using hylocereus costaricensis peel extract and their photocatalytic properties biosynthesis of copper nanoparticles using *Hylocereus costaricensis* peel extract and their photocatalytic properties, Karbala Int. J. Mod. Sci. 9 (2023) 289–306, https://doi.org/10.33640/2405-609X.3300.
[41] S.E. Putri, A. Ahmad, I. Raya, R.T. Tjahjanto, R. Irfandi, H. Karim, S.S. Desa, A. Rahman, The effect of thermal treatment on the characteristics of porous ceramic-based natural clay and chitosan biopolymer precursors, Indones. J. Chem. 23 (2023) 727, https://doi.org/10.22146/ijc.80375.
[42] S.E. Putri, D.E. Pratiwi, R.T. Tjahjanto, N.M. Ilyas, A. Rahman, H. Heryanto, Effect of sintering temperature on the microstructure behavior of gelcasted porous ceramics using cassava starch as pore template, Indones. J. Chem. 23 (2023) 1199–1211, https://doi.org/10.22146/ijc.78875.
[43] B. Ingham, M.F. Toney, 1 - X-ray diffraction for characterizing metallic films, in: K. Barmak, K. Coffey, eds., Met. Film. Electron. Opt. Magn. Appl., Woodhead Publishing. 2014, pp. 3–38, https://doi.org/10.1533/9780857096296.1.3.
[44] M.R. Mansor, Z. Mustafa, S.H.S.M. Fadzullah, G. Omar, M.A. Salim, M.Z. Akop, 3 - recent advances in polyethylene-based biocomposites, in: S.M. Sapuan, H. Ismail, E.S. Zainudin, eds., Nat. Fibre Reinf. Vinyl Ester Vinyl Polym. Compos., vol. 3, Woodhead Publishing. 2018, pp. 71–96, https://doi.org/10.1016/B978-0-08-102160-6.00003-2.
[45] R. Manurung, R.R. Syahputri Zuhri, H. Siregar, A.G. Agustan Siregar, Effect of K-Silica heterogeneous catalyst in transesterification reaction of crude palm oil, IOP Conf Ser Mater Sci Eng 1003 (2020) 012062, https://doi.org/10.1088/1757-899X/1003/1/012062.
[46] R. Cheula, M. Maestri, G. Mpourmpakis, Modeling morphology and catalytic activity of nanoparticle ensembles under reaction conditions, ACS Catal 10 (2020) 6149–6158, https://doi.org/10.1021/acscatal.0c01005.
[47] Z. Liu, J. Yuan, Z. Sun, X. Feng, Y. Liu, H. Zhu, C. Peng, C. Yang, Morphology effect on catalytic performance of ebullated-bed residue hydrotreating over $Ni–Mo/Al_2O_3$ catalyst: a kinetic modeling study, Green Chem. Eng. 10 (2022) 1–8, https://doi.org/10.1016/j.gce.2022.09.003.
[48] Sunardi Silviana, Synthesis and characterization of SiO_2/ZnO nanocomposites from zinc waste and mount Merapi volcanic ash, J Chem Appl 23 (2020) 365–369, https://doi.org/10.14710/jksa.23.10.365-369.
[49] A.P.S. Prasanna, K.S. Venkataprasanna, B. Pannerselvam, V. Asokan, R.S. Jeniffer, G.D. Venkatasubbu, Multifunctional ZnO/SiO_2 core/shell nanoparticles for bioimaging and drug delivery application, J Fluoresc 30 (2020) 1075–1083, https://doi.org/10.1007/s10895-020-02578-z.
[50] O. V Larina, P.I. Kyriienko, D.Y. Balakin, M. Vorokhta, I. Khalakhan, Y.M. Nychiporuk, V. Matolín, S.O. Soloviev, S.M. Orlyk, Effect of ZnO on acid–base properties and catalytic performances of $ZnO/ZrO_2–SiO_2$ catalysts in 1,3-butadiene production from ethanol–water mixture, Catal Sci Technol 9 (2019) 3964–3978, https://doi.org/10.1039/C9CY00991D.
[51] S.E. Putri, D.E. Pratiwi, R.T. Tjahjanto, Hasri, I. Andi, A. Rahman, A.I.W. Sari Ramadani, A.N. Ramadhani, Subaer,

A. Fudholi, The renewable of low toxicity gelcasting porous ceramic as Fe_2O_3 catalyst support on phenol photodegradation, Int J Des Nat Ecodyn 17 (2022) 503–511, https://doi.org/10.18280/ijdne.170403.

[52] S. Brunauer, L.S. Deming, W.E. Deming, E. Teller, On a theory of the van der Waals adsorption of gases, J Am Chem Soc 62 (1940) 1723–1732, https://doi.org/10.1021/ja01864a025.

[53] I.W. Khan, A. Naeem, M. Farooq, I.U. din, Z.A. Ghazi, T. Saeed, Reusable Na-SiO_2@CeO_2 catalyst for efficient biodiesel production from non-edible wild olive oil as a new and potential feedstock, Energy Convers Manag 231 (2021) 113854, https://doi.org/10.1016/j.enconman.2021.113854.

[54] K. Cholapandian, B. Gurunathan, N. Rajendran, Investigation of CaO nanocatalyst synthesized from *Acalypha indica* leaves and its application in biodiesel production using waste cooking oil, Fuel 312 (2022) 122958, https://doi.org/10.1016/j.fuel.2021.122958.

[55] M.L. Takeno, I.M. Mendonça, S. de S. Barros, P.J. de Sousa Maia, W.A.G. Pessoa, M.P. Souza, E.R. Soares, R. dos S. Bindá, F.L. Calderaro, I.S.C. Sá, C.C. Silva, L. Manzato, S. Iglauer, F.A. de Freitas, A novel CaO-based catalyst obtained from silver croaker (*Plagioscion squamosissimus*) stone for biodiesel synthesis: waste valorization and process optimization, Renew Energy 172 (2021) 1035–1045, https://doi.org/10.1016/j.renene.2021.03.093.

[56] S. de S. Barros, F.X. Nobre, W. V Lobo, S. Duvoisin Jr., C.A.S. de Souza, V.L. de Q. Herminio, I.H. Pereira, E.P. Silva, S. Iglauer, F.A. de Freitas, Eco-friendly biodiesel production using passion fruit peels and cupuaçu seeds: catalyst development and process optimization, Biofuels, Bioprod. Biorefining. 9 (2023) 1–17, https://doi.org/10.1002/bbb.2551.

[57] I.M. Mendonça, F.L. Machado, C.C. Silva, S. Duvoisin Junior, M.L. Takeno, P.J. de Sousa Maia, L. Manzato, F.A. de Freitas, Application of calcined waste cupuaçu (*Theobroma grandiflorum*) seeds as a low-cost solid catalyst in soybean oil ethanolysis: statistical optimization, Energy Convers Manag 200 (2019) 112095, https://doi.org/10.1016/j.enconman.2019.112095.

[58] F.A. de Freitas, I.R.S. Mendonça, S. de S. Barros, W.G.A. Pessoa, I.S.C. Sá, L.B. Gato, E.P. Silva, M.A.S. Farias, F.X. Nobre, P.J.S. Maia, S. Iglauer, K.K.Y. Isla, Biodiesel production from tucumã (*Astrocaryum aculeatum Meyer*) almond oil applying the electrolytic paste of spent batteries as a catalyst, Renew Energy 191 (2022) 919–931, https://doi.org/10.1016/j.renene.2022.04.083.

[59] B. Maleki, H. Esmaeili, M. Mansouri, D. Kumar, B. Singh, Enhanced conversion of dairy waste oil to biodiesel via novel and highly reactive UiO-66-NH_2/ZnO/TiO_2 nano-catalyst: optimization, kinetic, thermodynamic and diesel engine studies, Fuel 339 (2023) 126901, https://doi.org/10.1016/j.fuel.2022.126901.

[60] S. Tamjidi, B. Kamyab Moghadas, H. Esmaeili, Ultrasound-assisted biodiesel generation from waste edible oil using $CoFe_2O_4$@GO as a superior and reclaimable nanocatalyst: optimization of two-step transesterification by RSM, Fuel 327 (2022) 125170, https://doi.org/10.1016/j.fuel.2022.125170.

[61] S.E. Putri, D.E. Pratiwi, R.T. Tjahjanto, I. Andi, A. Rahman, I. Wulan, S. Ramadani, A.N. Ramadhani, A. Fudholi, The renewable of low toxicity gelcasting porous ceramic as Fe_2O_3 catalyst support on phenol, Photodegradation 17 (2022) 503–511, https://doi.org/10.18280/ijdne.170403.

[62] I.M. Mendonça, O.A.R.L. Paes, P.J.S. Maia, M.P. Souza, R.A. Almeida, C.C. Silva, S. Duvoisin, F.A. de Freitas, New heterogeneous catalyst for biodiesel production from waste tucumã peels (Astrocaryum aculeatum Meyer): parameters optimization study, Renew Energy 130 (2019) 103–110, https://doi.org/10.1016/j.renene.2018.06.059.

[63] S. Dehghani, M. Haghighi, Sono-enhanced dispersion of CaO over Zr-Doped MCM-41 bifunctional nanocatalyst with various Si/Zr ratios for conversion of waste cooking oil to biodiesel, Renew Energy 153 (2020) 801–812, https://doi.org/10.1016/j.renene.2020.02.023.